Carbon Isotopic Signatures of Individual Archean Microfossils(?) from Western Australia

YUICHIRO UENO,

Department of Earth and Planetary Sciences, Tokyo Institute of Technology, Tokyo 152-8551 Japan

YUKIO ISOZAKI,

Department of Earth Science and Astronomy, University of Tokyo, Meguro, Tokyo 153-8902, Japan

HISAYOSHI YURIMOTO, AND SHIGENORI MARUYAMA

Department of Earth and Planetary Sciences, Tokyo Institute of Technology, Tokyo 152-8551 Japan

Abstract

New types of carbonaceous filamentous microstructures have been identified in silica veins at two new localities in the ~3.5 Ga North Pole area of Western Australia. Their carbon isotopic compositions were measured *in situ* by secondary-ion mass spectrometry. The carbonaceous filaments are ~1 μm wide, 10 to 100 μm long, and are permineralized in a fine-grained (~1 μm) silica matrix. They are morphologically divided into three types (i.e., spiral, thread-like, and branched filaments). Their sizes and morphologies resemble modern and previously reported fossil bacteria. These similarities and their complex three-dimensional geometry suggest that they may represent morphologically preserved fossil bacteria. $\delta^{13}C$ values of the carbonaceous filaments range from –42 to –32‰, which strongly suggest that they are composed of biologically fixed organic compounds, possibly via the reductive acetyl-CoA pathway or the Calvin cycle. This is consistent with the hypothesis that autotrophs already existed on the Archean Earth.

Introduction

INFORMATION ABOUT THE early evolution of life on Earth has been obtained from the fossil record, and from the molecular phylogeny of extant organisms (e.g., Woese, 1987; Stetter, 1994; Schopf, 1998; Knoll, 1999). On the basis of the 16S rRNA sequence, the Universal Tree of Life has been formulated as a possible chart of evolutionary history of extant organisms. Age constraints on early biological evolution, however, depend on precise dating of sedimentary rocks containing recognizable microfossils (Schopf and Walter, 1983), including stromatolites (Walter, 1983), biomarker molecules (Brocks et al., 1999; Summons et al., 1999), and carbon isotopic distributions consistent with the presence of past life (Hayes, 1994; Mojzsis et al., 1996).

Among these various lines of evidence for early Archean life, the most robust is the occurrence of morphologically preserved and identifiable microfossils. Some previously reported Early Archean microstructures are recognizable as microfossils, but their poor state of preservation and relatively simple morphologies have raised endless doubts about identification and interpretation (Schopf and Walter, 1983; Buick, 1990).

To date, the oldest known microfossil on Earth occurs in the ~3.5 Ga North Pole–Marble Bar area in the Pilbara craton, Western Australia (Awramik et al., 1983; Schopf and Packer, 1987; Schopf, 1993). These oldest microfossils exhibit morphological variations, including septated filamentous, nonseptated filamentous, to coccoidal shapes (Awramik et al., 1983; Schopf and Packer, 1987; Schopf, 1993). In addition, nonseptated filaments occur in the ~3.4 Ga Hooggenoeg and Kromberg formations, Barberton Mountain Land, South Africa (Walsh, 1992). On the basis of morphology, some of these Early Archean filamentous microfossils resemble trichomic cyanobacteria (Schopf, 1993), suggesting that oxygenic photoautotrophs may have already existed in the Early Archean.

The recent finding of distinct biomarker molecules for cyanobacteria, 2α-methylhopanes from the ~2.7 Ga Jeerinah Formation in Western Australia (Brocks et al., 1999) supports the supposition that photoautotrophs had appeared in the Archean. Such molecules in Archean sedimentary rocks, however, generally have been degraded by thermal alteration,

and their primary signatures commonly have been lost (Summons and Hayes, 1992). Therefore, extraction and identification of biomarker molecules, particularly from Archean sedimentary rocks, involve great difficulties, and create uncertainties.

On the other hand, carbon isotopic signatures of Archean sedimentary rocks are promising, because they are little changed by post-depositional thermal processes (Schidlowski et al., 1983; DesMarais, 1997; Watanabe et al., 1997). Previous analyses of carbon isotopes of Archean sedimentary organic matter suggest that autotrophic organisms, which preferentially fix isotopically light carbon, e.g., using the "Rubisco" enzyme, may have appeared and become active by 3.5 Ga (e.g., Eichmann and Schidlowski, 1975; Hayes et al., 1983; Strauss and Moore, 1992).

Previously, these bulk carbon isotopic compositions were measured by conventional methods. However, the bulk isotopic compositions of sedimentary organic carbon are only inadequate indicators of carbon fixation reactions used by past autotrophic organisms, because sedimentary organic matter is generally composed of mixed remains of physiologically different microorganisms, each of which may have different carbon isotopic compositions. Recent advances in high-mass-resolution ion-microprobe techniques permit in situ analyses of carbon isotopic variations at the scale of <10 μm (e.g., Mojzsis et al., 1996). Application of this technique to ~850 Ma and ~2100 Ma microfossils by House et al. (2000) indicated autotrophic origins of the microfossils, which may have fixed inorganic carbon via the Calvin cycle. This approach is useful for deducing physiological aspects of morphological microfossils, and is also applicable even to much older Archean examples.

The purposes of this study are: (1) to measure in situ the carbon isotopic compositions of micron-scale organic material, including probable microfossils with the ion microprobe; this should constrain the carbon fixation pathway utilized by the past autotrophs; and (2) to identify morphologically preserved microfossils from the weakly metamorphosed Early Archean supracrustal rocks of the Pilbara craton, one of the most promising candidate areas on Earth.

Intensive field mapping and rock sampling were carried out in the North Pole area by more than 10 geologists, mainly from the Tokyo Institute of Technology in nine field seasons during the period 1991–2000. Full reports will be published in other arti-

cles. For microfossil research, more than 300 samples were cut into polished slabs and thin sections. As a result, we have identified about 100 carbonaceous filamentous microstructures at two new localities.

In this paper, we report the characteristics and mode of occurrence of the host rock together with morphotypes of the newly found filaments. In addition, we present the results of in situ carbon isotope measurements of these filaments, and discuss their paleobiological implications.

Geologic Setting

The northern part of the Pilbara craton in Western Australia is underlain by an Archean granite-greenstone terrane (Fig. 1). The greenstone belt of the terrane is composed mainly of altered basaltic greenstones associated with minor felsic volcanics and sedimentary rocks including chert, mudstone, sandstone, and conglomerate. These volcano-sedimentary rocks have been grouped together into the Pilbara Supergroup (Hickman, 1983, 1990). Zircon U-Pb dating has yielded 3.5 to 2.9 Ga for the Supergroup (Thorpe et al., 1992b). The oldest known microfossils were reported (Awramik et al., 1983; Schopf and Packer, 1987; Schopf, 1993) from chert beds of the Warrawoona Group that belong to the lower part of the Pilbara Supergroup. The Warrawoona Group (apparently >10 km thick) is composed mainly of basaltic greenstones with intercalated siliceous sedimentary rocks and felsic volcanics. This group unconformably overlies the lithologically similar Coonterunah Group (Hickman, 1983; Van Kranendonk, 1999).

The North Pole area in the Pilbara craton, the locality of the oldest microfossils (Awramik et al., 1983), is located nearly 160 km south of Port Headland, and about 50 km west of Marble Bar (Fig. 1). In the North Pole area, the lower to middle part of the Warrawoona Group crops out (Lipple, 1975; Hickman, 1983), and consists of ~6 km thick basaltic greenstones intercalated with 1 to 70 m-thick bedded chert in three units (Fig. 2; Isozaki et al., 1997). Among the three, the lowermost chert unit is 1 to 70 m thick, and is intercalated with several barite beds of 0.1 to 5 m thickness. This chert unit associated with barite corresponds to the "chert-barite unit" described by Buick and Dunlop (1990). The well-known microfossils occur in this unit (Awramik et al., 1983). The other two chert units are thinner
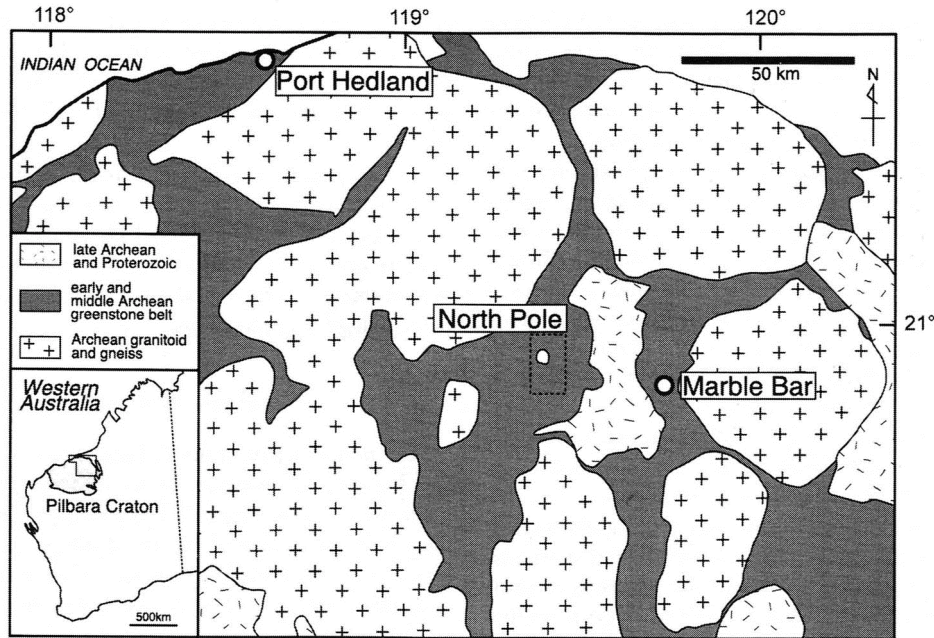
FIG. 1. Index map of the North Pole area of the Pilbara craton (modified after Hickman, 1990). Study area is shown by a dashed frame (Fig. 2).

(1–13 m) than the chert-barite unit, and are rarely associated with barite.

The precise age of the chert-barite unit has never been dated directly. Zircon U-Pb dating yields an age of 3458 ± 2 Ma for the felsic volcanics (Thorpe et al., 1992b) that overlie the cherts and greenstones in the North Pole area. This means that the age of the chert-barite unit is older than 3.46 Ga.

In the North Pole area, numerous (>1600 identified) silica veins have intruded into the greenstones (Fig. 2). They are 0.3–20 m wide and generally >100 m long, with the longest over 1 km. The veins are massive and are mainly composed of chert-like, fine-grained silica (~1 µm). They were previously called T-chert (Dunbar and Rodgers, 1961). However, we use the term silica vein instead of T-chert, because "chert" is a term appropriate for a sedimentary rock.

Most of the silica veins occur in the greenstones below the chert-barite unit (Fig. 2). In some cases, they intrude chert beds of the chert-barite unit, but the veins do not cut through the entire unit, nor into the overlying pillow basalt. The tops of the silica veins show gradual transition into certain chert beds, forming a clear T-junction, as shown in Figure 3. These relationships suggest that the silica veins

were formed intermittently during the deposition of chert beds of the chert-barite unit, a conclusion also arrived at by Isozaki et al. (1997) and Nijman et al. (1998). Alternatively, Buick (1984, 1988, 1990) hypothesized that the silica veins extruded upward as sills into overlying chert beds. Also from regional tectonic relationships, he concluded that the veins were emplaced in the period 3400–2750 Ma. Thus the age of the silica veins is as old as the Archean, and possibly goes back to ca 3.5 Ga, as discussed in detail later.

Description of the Silica Veins

The newly found carbonaceous filaments at two localities—named Locality 1 (Australian Map Grid 2755-519563) and Locality 2 (2755-534654)—are both from the chert-barite unit shown in Figure 2. The two are ~10 km apart, but our detailed mapping enabled them to be correlated at the same stratigraphic horizon.

Locality 1

Here, a black silica vein, 1–2 m wide has intruded ~20 m thick bedded cherts interstratified with barite. These bedded cherts are divided into
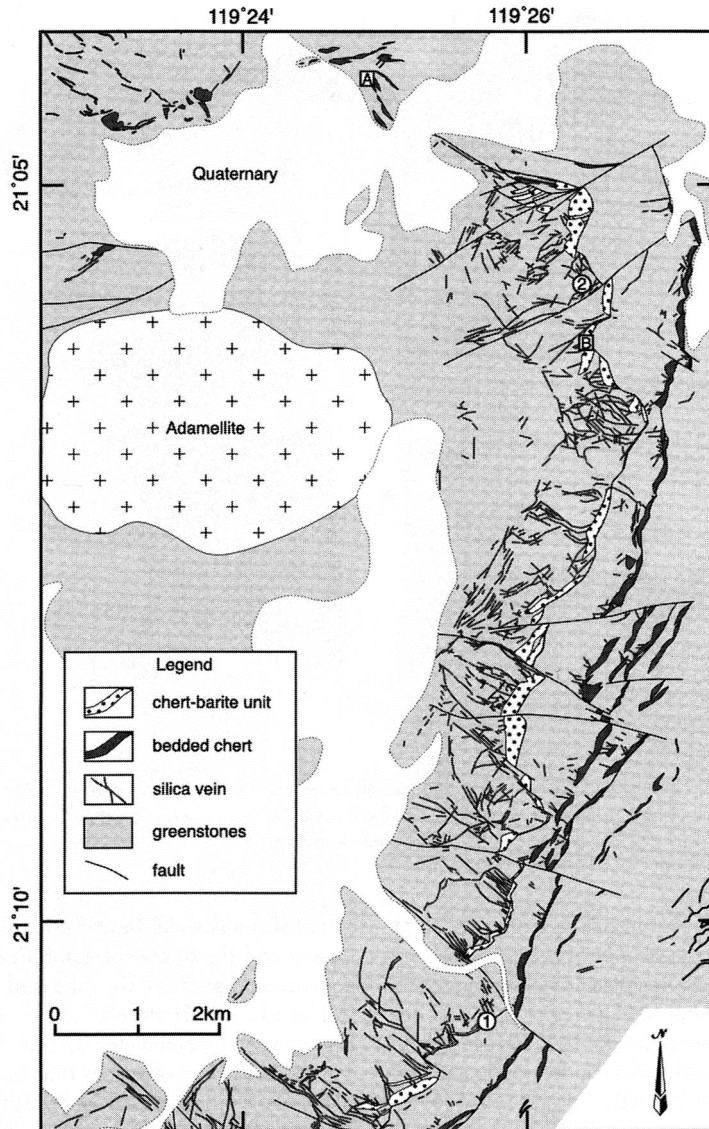
FIG. 2. Lithologic map of the North Pole area (modified after Isozaki et al., 1997). The numbers 1 and 2 indicate Localities 1 and 2, respectively (see text). The letters A and B indicate previously reported microfossil localities, corresponding to locality A and locality B of Awramik et al. (1983).

two parts—Chert A and overlying Chert B (Fig. 3). Chert A is composed of 2–3 cm thick, black, grey, and/or white bedded chert and 5–10 cm thick bedded barite. Chert B is composed of 0.3–0.5 m thick, light green to reddish grey, bedded chert.

The silica vein clearly cuts the bedding surfaces of Chert A and also penetrates into Chert A as an apophysis, whereas it is depositionally overlain by Chert B. The top of the silica vein shows a gradual transition into the bottom bed of Chert B. The carbonaceous filaments were found from the black silica rock of the vein nearly 10 m below the bottom surface of Chert B.

The silica vein is mainly composed of fine-grained (~1 µm) silica, which encloses smaller amount of kerogen-rich clasts, kerogen clots, pyrite-
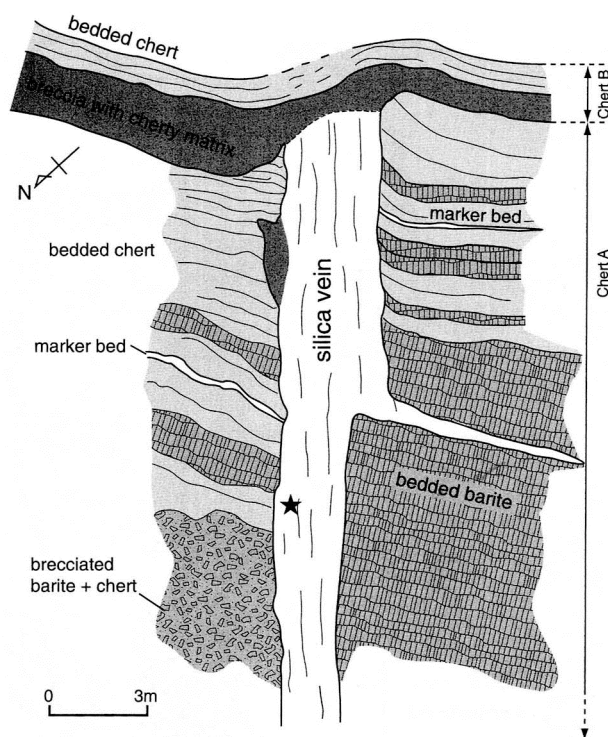
FIG. 3. Mode of occurrence of the fossil-bearing black silica vein at Locality 1. This diagram shows that the silica vein intruded the chert/barite beds of the North Pole chert-barite unit. Note that Chert A is cut by the silica vein, whereas Chert B covers the vein. The star symbol indicates the sample locality of 96NP452.

sphalerite-dominated sulfides, and carbonates (Fig. 4E). The angular kerogen-rich clasts, typically ~1 cm across, are themselves also composed mainly of fine-grained silica with kerogen clots, sulfides, and carbonates. The fine-grained silica, kerogen clots, and sulfides are in turn cross-cut by quartz and barite veinlets (Figs. 4A and 4B).

Locality 2

A 3 m wide silica vein occurs here in the middle of pillowed greenstones. The carbonaceous filaments occur in a black silica vein, which is located nearly 80 m below the bottom surface of the overlying chert beds. The lithology of the silica vein at this locality is identical to that at Locality 1.

Carbonaceous Filaments

In order to determine mineralogical compositions, a scanning electron microscope (JEOL JSM5310) with an X-ray analysis system (Oxford Link ISIS) was used. In addition, inorganic mineral phases and the degree of graphitization of the carbonaceous material (Wopenka and Pasteris, 1993; Yui et al., 1996) were determined with a laser Raman spectrophotometer (JASCO NRS-2000).

About 100 carbonaceous filaments are preserved in the black silica veins from Localities 1 and 2. The filaments, ~1 μm wide and >10 μm long, are permineralized in a fine-grained silica matrix with kerogen-rich clasts, kerogen clots, and sulfides (Figs. 4E and 4F). The filaments also occur within the kerogen-rich clasts. More than 50 filaments occur in each thin section (~10 cm^2). The filaments and kerogen clots do not occur in the later, cross-cutting quartz and barite veinlets (Fig. 4B).

The filaments are composed of black carbonaceous material (Fig. 5). The D(disordered-)/O(ordered-) peak area ratios of their Raman spectra would correspond to an in-plane crystallite size smaller than 50 Å (Wopenka and Pasteris, 1993). This fact, as well as their D/O peak intensity ratios
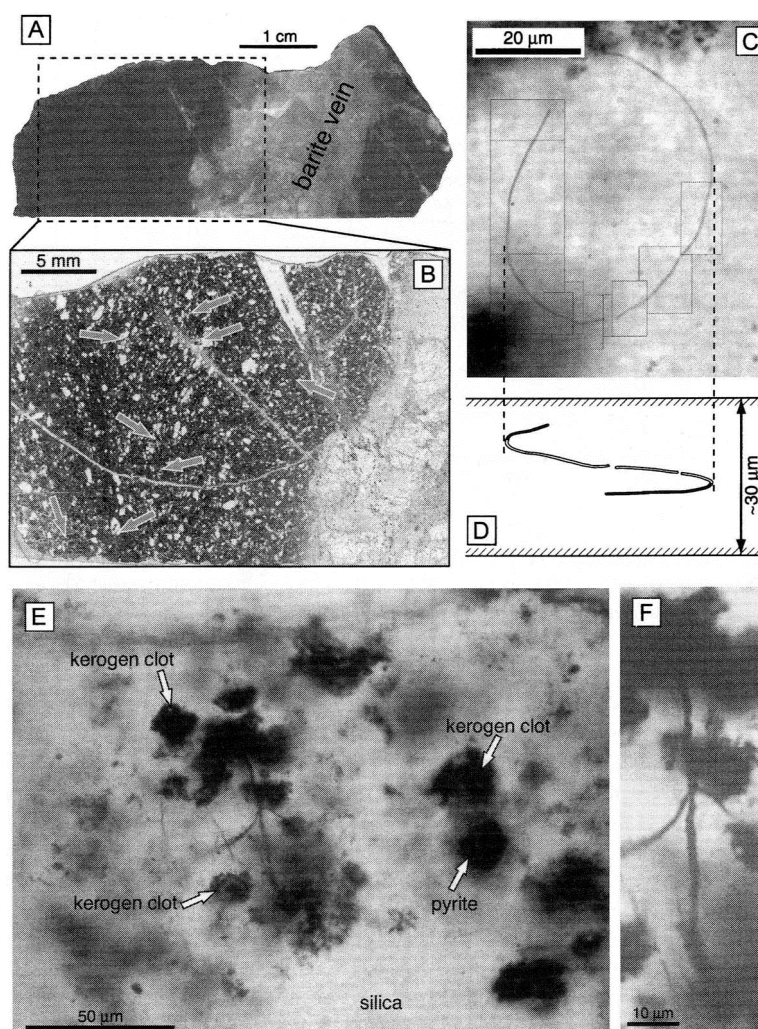
FIG. 4. Photographs of the silica vein. A. Cut-surface of the silica vein sample 96NP759. Dashed frame refers to Figure B. B. Petrographic thin section of 96NP759. Black part is occupied by kerogen clots, sulfide, and fine-grained silica. Note that the carbonaceous filaments (indicated by arrows) are scattered in the silica matrix. C. Optical photomontage at 11 different focal depths shows a thread-like filament in sample 96NP759. D. Interpretive diagram of the cross section of the ~30 μm thick thin section shows three-dimensional geometry of the filament of Figure C. E. Optical photomicrograph shows mode of occurrences of kerogen clots and carbonaceous filaments. F. Magnification view of Figure E.

from 1.0 to 1.4 and D peak width (i.e., full width at half maximum) from 60 to 90 cm^{-1}, indicate that their degree of graphitization reached the lower greenschist facies (Yui et al., 1996). This Raman spectral feature of the filaments is nearly identical to those of the kerogen clots from the samples.

Some individual filaments have three-dimensional geometries, such as spiral forms (Figs. 6E–6G), and do not lie in a single plane (Figs. 4C and 4D). Some filaments show a radiating arrangement from holdfast-like kerogen clots (Fig. 6B) or from the wall of kerogen-rich clasts (Fig. 6C). Several filaments are also bunched and mutually interwoven (Figs. 6B and 6C). The filaments are morphologically divided into spiral, thread-like, and branched filaments.
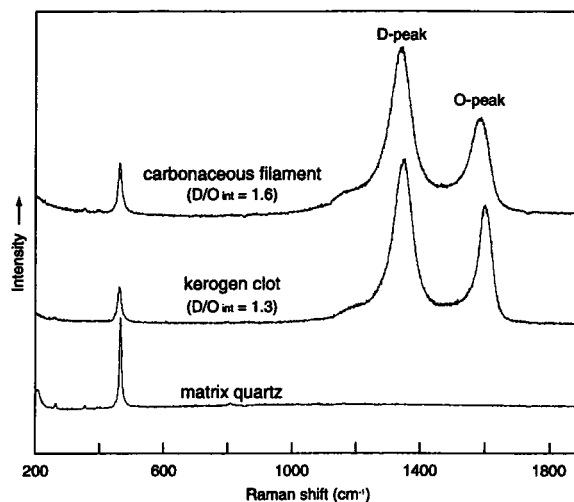
FIG. 5. Representative Raman spectra of a carbonaceous filament (top), kerogen clot (middle), and matrix quartz (bottom). O-peak (near 1600 cm^{-1}) and D-peak (near 1355 cm^{-1}) are from carbonaceous material. The microscope objective used is 100x; thus the analytical spot size is ~1 μm. Details of Raman analytical procedures are given in Wopenka and Pasteris (1993).

Spiral filaments (Figs. 6E–6G) are 0.2 μm to 1.8 μm in width (most ~1 μm, average 0.6 μm; n = 10) and more than 30 μm in length, with spiral morphology as a whole. The diameter of individual filaments is constant. The diameter of the spire is less than 5 μm.

Thread-like filaments are subdivided into two types according to their different widths. Narrow ones (Figs. 4C, 4D, 6A, and 6H) are 0.1 to 0.8 μm wide (most 0.3 μm, average 0.4 μm; n = 54) and 10 μm to >100 μm long. Broad ones (Figs. 6C and 6I) are 1.0 μm to 1.8 μm wide (most 1.4 μm, average 1.3 μm; n = 7) and 20 to 100 μm long. Narrow ones show elongated rod–shapes. The diameter of individual filaments is constant, and they display gently curved morphologies without branching, with a rounded terminal shape (Fig. 6A). They apparently have no septa-like structure. Broad filaments are mostly rectilinear; some are curvilinear. Most broad forms have rough surfaces (Figs. 6C and 6I).

Branched filaments (Fig. 6B) are 0.2 to 0.4 μm wide (n = 3) and ≥20 μm long. Filaments branch into two filaments of the same width.

Carbon Isotope Analysis

Analytical techniques

In order to evaluate the origin of the carbonaceous filaments, we performed in situ measurement of the carbon isotopic composition of the filaments and kerogen clots from the two rock samples mentioned above (96NP452 and 96NP759 from Localities 1 and 2, respectively). After microscopic observation, the filament-bearing domains in the thin sections were cut into small chips (6 mm × 6 mm). These were polished with alumina powder, ultra-sonically cleaned in distilled water and then in ethanol, and then coated with ~40 nm thick Au film.

Carbon isotopic measurements were performed by secondary-ion-mass spectrometry (SIMS) using a CAMECA IMS1270 at the Tokyo Institute of Technology. Gold-coated carbonaceous materials in thin section were sputtered by a focused 20 keV Cs$^+$ primary beam. Measurements of ^{12}C$^-$ and ^{13}C$^-$ secondary ions were made under a high-mass-resolution mode (M/ΔM = ~4500) in order to separate the ^{12}CH$^-$ interference at mass 13. A normal-incident electron flood gun was utilized to compensate electrostatic charging of the analysis area by the Cs$^+$ sputtering. The primary beam was focused into a small spot (<10 μm) and a field aperture (2 × 2 mm^2) was inserted into the secondary ion optics. A 150 μm field setting for the transfer optics was used. Secondary ions were collected through an energy window of ±75 eV. Constant count rates of 4 × 10^5 cps and 3–4 × 10^5 cps of ^{12}C$^-$ were maintained to eliminate uncertainties in dead-time correction of the electron multiplier pulse counting system for
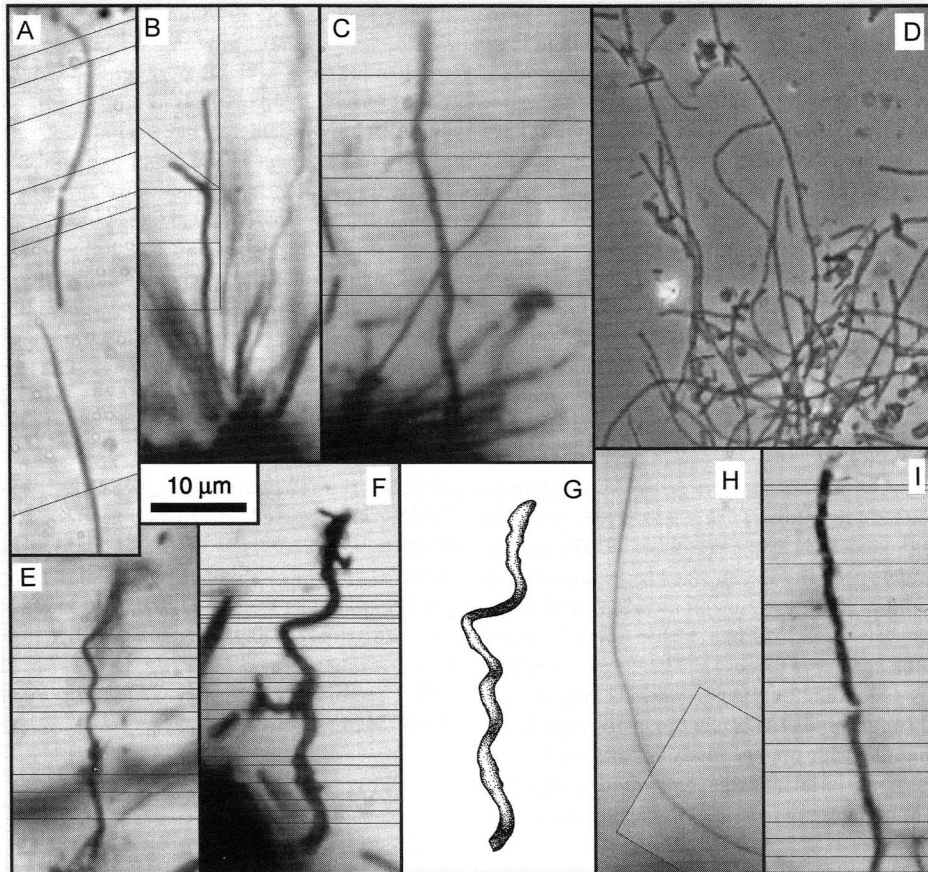
FIG. 6. Optical photomicrographs of carbonaceous filaments from the black silica vein at Locality 1 (Figs. C, E, F, and H), Locality 2 (Figs. A, B, and H), and modern example (Fig. D). A. Thread-like filament. B and C. Aggregate of filaments radiating from the holdfast-like kerogen clots. D. Living examples of filamentous bacterium belonging to the phylum of the *Aquifex-Hydrogenobacter* complex from sulfur-turf microbial mats of Nakanoyu Hot Spring, Japan (Yamamoto et al., 1998; Hiraishi et al., 1999). E and F. Spiral filaments. G. Schematic reconstruction of spiral filament shown in Figure E. H and I. Thread-like filament. Figs. A, B, C, E, F, H, and I are photomontages at 8, 5, 9, 12, 24, 2, and 15 different focal depths, respectively. Scale bar is 10 μm for all figures.

standard and unknown, respectively. Dead-time of the counting system was 21.2 ± 0.8 and 28.1 ± 2.4 ns in 1998 and in 2000, respectively, because of exchange of the electron multiplier. These count rates were achieved with a primary beam current of $3 \text{ pA} - 1 \text{ nA}$. Signals of $^{12}C^-$ and $^{13}C^-$ were accumulated for 2 and 5 seconds, respectively, during each cycle. The carbon isotopic composition was usually determined by averaging the ratios of $^{13}C^-/^{12}C^-$ from 100 data cycles.

The $^{13}C^-/^{12}C^-$ ratios, after the correction of dead-time and of instrumental mass fractionation, are reported as a $\delta^{13}C$ value relative to the $^{13}C/^{12}C$ ratio

of the Chicago PDB standard ($^{12}C/^{13}C = 88.99$; Craig, 1957). Instrumental mass fractionation was corrected using the USGS24 graphite standard ($\delta^{13}C_{PDB} = -15.90 \pm 0.25 \text{ ‰}$) mounted on a separate glass plate. The standard and unknown samples were set in the same sample holder. Measurements of this standard were performed several times at the beginning, during, and at the end of each analytical session. The procedure of mass fractionation correction assumes that the degree of bias for the lighter isotope inherent in the sputtering process is the same for the sample as for the graphite standard. In most analyses, the focused beam overlapped car-

bonaceous materials and the surrounding silica. However, secondary C⁻ ions were only emitted from the carbonaceous material because the surrounding silica was C-free. Where the targets were smaller than the primary beam size, the emitted secondary carbon ion intensities often changed during the analysis. This is because the irradiated target area changes by sputtering. The variations of the ^{12}C⁻ intensities for the standard and unknown samples were less than 25% of the average intensity except for the case of the 452f3, 452f4, 452f5, 452f6, 759f01, and 759f02 analyses. The ^{12}C⁻ intensities of the 452f3, 452f4, 452f5, 452f6, 759f01, and 759f02 analyses changed from 25 to 60% of the average intensities. This effect was corrected by quadric time interpolation.

The analyses were performed in four independent analytical sessions (three analyses were in 1998 and one was in 2000; see Table 1). The degree of variation in instrumental mass fractionation was within about ±7‰ among independent analytical sessions. The variation was within ±3‰ in each analytical session (Table 1). The large variation among independent analytical sessions may be due to small conditional changes in the instrumental setting. Therefore, for precise analysis, the instrumental mass fractionation was corrected using the fractionation factor determined in each session.

Results

The results of the analyses are listed in Table 1. Carbon isotopic compositions were determined for 7 and 2 carbonaceous filaments, and 12 and 5 kerogen clots from sample 96NP452 and 96NP759, respectively. The 2 filaments and 5 clots from 96NP759 are in one thin section, TS-4, whereas the 7 filaments and 12 clots from 96NP452 are present in three different thin sections, TS-1, TS-2, and TS-3, which include six (i.e., NP452a, NP452b, NP452c1, NP452c2, NP452d, and NP452e), seven (i.e., 452CM1, 452CM2, 452f1, 452f3, 452f4, 452f5 and 452f6), and six (i.e., 452k01, 452k02, 452k03, 452k04, 452s01, and 452s02) analyzed domains, respectively. The actual distance between the TS-1 and TS-3 was ~10 cm within the same rock specimen, and TS-2 is located between the two.

Nine domains (i.e., 452f1, 452f3, 452f4, 452f5, 452f6, 452s01, 452s02, 759f01, and 759f02) that include carbonaceous filaments were analyzed. Among the nine, two domains (i.e., 452s01 and 452s02) included the same spiral filament (Fig. 7), whereas the other seven included thread-like fila-

ments. Five analyzed domains (i.e., 452f1, 452f3, 452f4, 452f5, and 452f6) are concentrated within a small area (about 100 μm × 100 μm) in the thin section, and include filaments radiating from a kerogen clot ~20 μm in diameter. In the sputtered craters of 452f1, one filament is included, and in 452f6, two filaments are included. These filaments are separated from the kerogen clot. Hence, the contribution of carbon from the kerogen clot to these analyses was insignificant. Three other domains (i.e., 452f3, 452f4, and 452f5) include several filaments and a kerogen clot. The obtained $\delta^{13}C_{PDB}$ values of these filaments are −42.1 to −32.2‰. The average $\delta^{13}C_{PDB}$ value of spiral filament (−37.5‰) is identical to that of thread-like filament (−36.0‰) within analytical error.

Seventeen domains (i.e., NP452a, NP452b, NP452c1, NP452c2, NP452d, NP452e, 452CM1, 452CM2, 452k01, 452k02, 452k03, 452k04, 759k01, 759k02, 759k03, 759k04, and 759k05) of the kerogen clots were analyzed. The kerogen clots vary in size (5 to 200 μm in diameter). Their average $\delta^{13}C_{PDB}$ values are −39.1‰ (S.D. = 2.5, n = 12) and −34.7‰ (S.D. = 3.3, n = 5) for 96NP452 and 96NP759, respectively.

Discussion

Here we discuss first the age of the filament-bearing silica veins, and then the morphology of the carbonaceous filaments. Finally, paleobiological implications of the carbon isotope measurements will be discussed.

Timing of consolidation and emplacement of the filament-bearing silica veins

All the detected carbonaceous filaments reported here are permineralized in the fine-grained silica matrix with kerogen clots and sulfides (Figs. 4E and 4F). They never occur in secondary mineral phases such as in barite and quartz veins (Figs. 4A and 4B). Thus we conclude that the filaments were embedded *in situ* within the silica veins at the time of their consolidation, not at a later stage.

Although the age of the silica veins containing the carbonaceous filaments has never been directly determined, Buick (1984, 1988, 1990) suggested that they were emplaced some time between 3400 and 2750 Ma on the basis of their regional tectonic relationships. On the other hand, Nijman et al. (1998) demonstrated transitional contacts between the veins and the chert-barite unit, and they con-

TABLE 1. Summary of Carbon Isotopic Compositions

Standard	$F^{13}C^1$, ‰	CM^2	$\delta^{13}C_{PDB}{}^4 \pm \sigma_m$, ‰	Filaments[3]	$\delta^{13}C_{PDB}{}^4 \pm \sigma_m$, ‰
		11/19/98 session (TS-1)			
		NP452a	−40.5 ± 1.8		
USGS24	−25.8 ± 1.7	NP452b	−39.4 ± 1.8		
		NP452c1	−42.3 ± 2.0		
		NP452c2	−39.1 ± 1.8		
		NP452d	−39.9 ± 1.8		
		NP452e	−40.0 ± 1.8		
		12/2/98 session (TS-2)			
USGS24	−24.6 ± 2.6	452CM1	−42.4 ± 2.8	452f1	−42.1 ± 2.6
		452CM2	−40.8 ± 2.6		
		12/9/98 session (TS-2)			
				452f3	−36.0 ± 1.9
USGS24	−33.4 ± 1.6			452f4	−33.1 ± 1.7
				452f5	−32.3 ± 1.7
				452f6	−36.1 ± 1.6
		5/10/00 session (TS-3 and TS-4)			
		452k01	−38.1 ± 2.2	452s01	−36.3 ± 2.3
USGS24	−19.6 ± 2.1	452k02	−34.6 ± 2.2	452s02	−38.7 ± 2.3
		452k03	−34.8 ± 2.2		
		452k04	−37.4 ± 2.2		
		759k01	−37.7 ± 2.2	759f01	−32.2 ± 2.4
		759k02	−35.0 ± 2.2	759f02	−40.5 ± 3.2
		759k03	−37.9 ± 2.2		
		759k04	−30.5 ± 2.2		
		759k05	−32.3 ± 2.3		

[1]Instrumental mass fractionation factors relative to $^{13}C/^{12}C$ isotope ratio of PDB ($^{12}C/^{13}C = 88.9$; Craig, 1957). Errors denote standard deviation of reproducibility among several independent analyses during the day.
[2]Kerogen clots in the black silica vein sample 96NP452 and 96NP759.
[3]Carbonaceous filaments in the black silica vein sample 96NP452 and 96NP759.
[4]Corrected $\delta^{13}C$ values relative to PDB. Errors, σ_m, are calculated from error propagation of the estimated standard deviations of the mean for the sample and standard deviation of reproducibility for standard of the day. The standard deviations of the mean for the sample are estimated by statistical fluctuation of secondary ions. Combined data of three analyses for 452f1, two for 452f3, six for 452f4, two for 452f5, and two for 452f6.

cluded that the vein formation was synchronous with the sedimentary deposition. These authors further suggested that, because the chert-barite unit has an acceptable age at least of 3458 Ma (Thorpe et al., 1992b), the silica veins must have a similar age.

Our observations confirm the conclusion of Nijman et al. (1998). At Locality 2, the silica vein is cross-cut by a barite vein with a sharp boundary (Fig. 4A), suggesting that lithification of the silica

vein was complete before barite precipitation. A model lead age of 3490 Ma was reported for galena in a vein barite within 10 km from our Locality 2 (Richards et al., 1981; Thorpe et al., 1992a). This age may possibly represent the minimum age of emplacement and lithification of the silica vein that contains the carbonaceous filaments. In summary, although the age of the filament-bearing silica vein is not yet tightly constrained, stratigraphic relation-
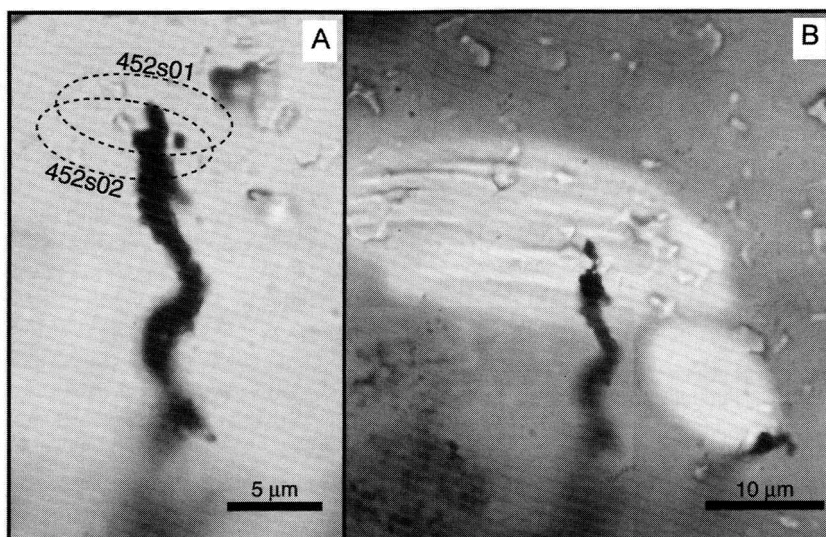
FIG. 7. A. Optical photomontage of spiral filament at three different focal depths before ion microprobe analysis. Dashed circles indicate the analysis domains. B. Optical photomontage showing the same filament of Figure A at two different focal depths after the analysis. Lighter domain amid darker surroundings indicates the area sputtered by Cs$^+$ ion.

ships with overlying 3458 Ma felsic volcanics (Thorpe et al., 1992b) suggest that this is a minimum age.

Morphology of the carbonaceous filaments

The conclusion that the carbonaceous filaments we have analyzed are morphologically preserved microfossils is equivocal, because of their simple morphologies. Notwithstanding, their morphologies are similar to those of Archean and Proterozoic microfossils as well as those of modern filamentous bacteria (Fig. 6D).

The filaments with various morphologies, such as spiral, bunched, and branched, are comparable in both size and morphology to those exhibited by modern bacteria (e.g., Buchanan and Gibbons, 1974; Brock, 1979; Holt et al., 1994) and by fossil bacteria including Archean (e.g., Awramik et al., 1983; Schopf and Walter, 1983; Schopf, 1992; Walsh, 1992) and Proterozoic examples (e.g., Barghoorn and Tyler, 1965; Schopf, 1968; Licari, 1978).

Particularly, our narrow thread-like filaments are identical to *Archaeotrichion contortum* (Schopf, 1968) in their apparently non-septate, unbranched, sinuous, gently curved morphology, their cross-section diameter (~0.3 μm), and solitary occurrence.

The thread-like filaments also are comparable to many modern filamentous bacteria such as *Methanobacterium thermoautotrophicum*, *Chloroflexus aurantiacus*, *Oscillatoria angustissima*, etc.

Some filaments radiate from holdfast-like kerogen clots. This aggregate of filaments is similar to previously reported *Warrawoonella radia*, which is interpreted only as a "possible microfossil" from the North Pole area (Awramik et al., 1983, 1988; Buick, 1984, 1988, 1990), as well as to modern rosette-forming bacteria such as *Thiothrix* and *Leucothrix*. Spiral filaments have never been previously reported from Archean strata, although their morphology and size (~1 μm in width) resembles those exhibited by modern bacteria and Proterozoic microfossils (Licari, 1978; Brock, 1979; Holt et al., 1994). The branching of some filaments is similar to that exhibited by several modern bacteria such as *Galionera* (Holt et al., 1994).

These similarities in the size and morphology of our filaments and modern bacteria, their carbonaceous compositions, and occurrence with others of similar morphology all suggest that they may be morphologically preserved fossil bacteria. Although migration of organic matter accompanied by mineral growth or migration along cracks or fissures can pro-

duce abiogenic microfossil-like carbonaceous filaments (Buick, 1984, 1988, 1990), it is unlikely that these processes could produce all of the morphologies of the filaments reported here. Some of the filaments have relatively complex three-dimensional geometries, which are not controlled by inorganic mineral shapes. The geometry of the spiral filaments (Figs. 6E–6G) and helically curved thread-like filaments (Figs. 4C and 4D) cannot be depicted in a single two-dimensional plane, and it is unlikely that they could have grown along individual cracks or multiple micro-fissures. Thus, we consider that the original filamentous structures were permineralized in their silica matrix. The apparent cellular feature and hollow nature discussed by Buick (1990) and Schopf and Walter (1983) was not detected. Condensation of organic walls resulting in a granular appearance of filamentous microfossils may explain this feature, as proposed by Knoll et al. (1988). Because the optical resolution was limited for the narrow (< ~1 μm wide) filaments, we could not determine whether the filaments are hollow or not. Further observation at higher resolution is necessary to detect cellular features and confirm their biogenicity. We have been careful to consider the carbonaceous filaments simply as "probable microfossils." Regardless of their biogenicity, however, it is clear that many carbonaceous filaments are contained in Archean silica veins, with ages possibly ranging down to ~3.5 Ga.

Carbon isotopic signatures

The $\delta^{13}C$ values of the filaments and kerogen clots measured in two samples range from −42.4 to −30.5‰. These results strongly point to a biogenic origin, because the values are too low to be derived from inorganic carbon compounds. The $\delta^{13}C$ value of sedimentary carbonate of the North Pole chert-barite unit is ~0‰ (Hayes et al., 1983), which is nearly equal to that of modern marine carbonate. Thus, the carbon isotopic fractionation between the carbonate and the carbonaceous material including the filaments themselves is 30–40‰. In the modern environment, ^{13}C-depleted organic material is produced essentially by autotrophic carbon fixation. It is unrealistic to consider that such a large fractionation was attained by non-biological processes (Schidlowski et al., 1983; Mojzsis et al., 1996).

Eiler et al. (1997) pointed out the possibility that Rayleigh distillation can modify isotopic compositions under metamorphic conditions and produce such ^{13}C-depleted carbonaceous material. However,

the following evaluation of this possible isotopic modification suggests that primary $\delta^{13}C$ values of the carbonaceous materials in the two silica veins may have been a few per mil lower than the values obtained here. According to this theoretical model, the magnitude and direction of the isotopic modification depend both on temperature and on relative proportion of devolatilized CO_2 and CH_4 (Fig. 8). The maximum temperature they have experienced can be assumed to be ~350°C, because the metamorphic grade of the greenstones in the studied area is generally in the prehnite-pumpelleyite to lowermost greenschist facies (Dunlop and Buick, 1981). This petrological result is consistent with the graphitization degree of the carbonaceous filaments deduced from their Raman spectra (Fig. 5).

Moreover, the carbonaceous filaments co-exist with pyrite but not with Fe-oxide, suggesting low oxygen fugacity of the hypothetical devolatilized fluid, which may have been enriched in CH_4 relative to CO_2 (Ohmoto and Kerrick, 1977). Under conditions of 350°C and a CO_2/CH_4 mole ratio = 1 (Fig. 8A), even if an unrealistically extensive 99% devolatilization (i.e., $f = 0.01$) is assumed, the remaining carbonaceous material is enriched in ^{12}C only by ~2‰ relative to the initial $\delta^{13}C$ value. In fact, lower temperature (< 350°C) and a lower CO_2/CH_4 mole ratio (< 1) would be more plausible (Figs. 8A and 8B). Under such conditions, a hypothetical Rayleigh distillation process raised their $\delta^{13}C$ values. Consequently, if it is assumed that this process modified the isotopic composition of the carbonaceous filaments, their $\delta^{13}C$ values represent the maximum of the original values. Furthermore, the modification beyond a few per mil is unlikely, because their high organic carbon concentrations (2.63 and 6.72 mgC/g for 96NP452 and 96NP759, respectively; Ueno et al., in prep.) relative to modern organic-rich sediment suggest that loss of carbon may have not been significant (viz., the f value is near 0).

Another possible cause of post-depositional isotopic modification is isotope exchange between carbonate and organic carbon. The $\delta^{13}C$ values of the carbonaceous material could have been raised by isotope exchange with isotopically "heavy" carbonate. However, field and experimental studies (e.g., Hoefs and Frey, 1976; Scheele and Hoefs, 1992) suggest that this isotope exchange reaction apparently does not occur below 350°C. Moreover, under such low-grade metamorphism or diagenesis, organic matter generally is enriched by only a few per mil in ^{13}C through the graphitization process
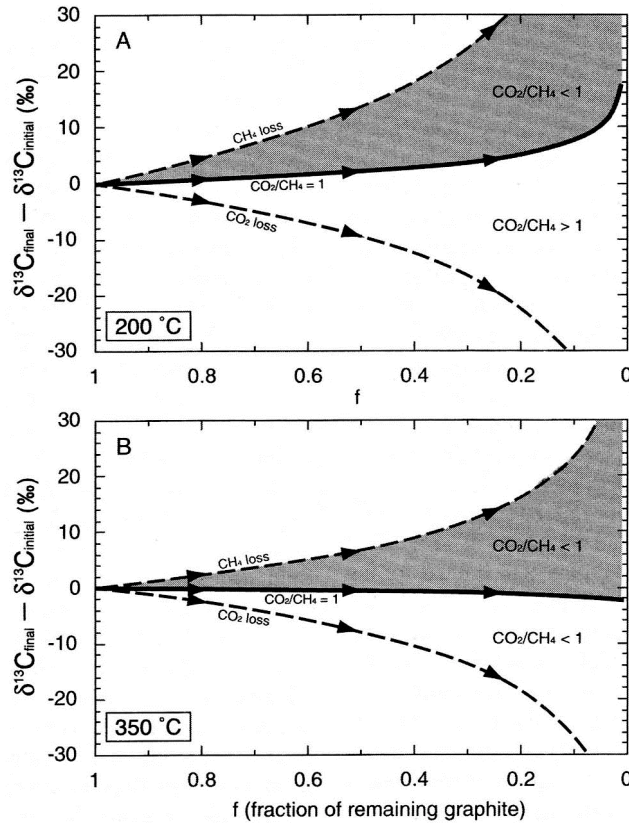
FIG. 8. Calculated changes in the $\delta^{13}C$ values of organic carbon (graphite) due to loss of CO_2- and CH_4-bearing fluids. These changes are evaluated by a Rayleigh distillation model (Eiler et al., 1997): $\delta^{13}C_{final} = (\delta^{13}C_{initial} + 1000) \times f^{(\alpha - 1)} - 1000$, where f refers to the fraction of carbon remaining and a is the fractionation factor between the released carbon species and residual graphite. The $\alpha_{CO2\text{-}graphite}$ values are 1.0139 and 1.0116 at 200 and 350°C, respectively, and the $\alpha_{CH4\text{-}graphite}$ values are 0.9801 and 0.9899 at 200 and 350°C, respectively (Chacko et al., 1991).

(Degens, 1969; Peters et al., 1981; DesMarais, 1997).

On the basis of the above discussion, we conclude that the measured $\delta^{13}C$ values of the carbonaceous material reported here may be nearly equal to or a few per mil higher than the primary $\delta^{13}C$ values. This assumption enables us to constrain the carbon fixation pathway, by which the minute carbonaceous material that includes the probable microfossils was synthesized. This is because various known carbon fixation pathways exhibit different degrees of isotopic fractionation (Schidlowski et al., 1983; Fuchs, 1989; House et al., 2000), and the expected maximum fractionation of each pathway can be experimentally determined (e.g., Padue et al., 1976; Farquhar et al., 1989; Laws et al., 1995;

Popp et al., 1998), even though the degree of fractionation can also depend on various parameters such as temperature, pH, salinity, growth rate of cell, and CO_2 availability.

The $\delta^{13}C$ values of the filaments (–42 to –32‰) in this study (Fig. 9) agree well with those exhibited via the reductive acetyl-CoA pathway (Fuchs et al., 1979; Preuss et al., 1989), and are consistent with those of some autotrophic bacteria utilizing the Calvin cycle (Sirevåg et al., 1977; Ruby et al., 1987; Preuss et al., 1989). Despite the disputable origin of the filaments, it is notable that some modern bacteria such as M. thermoautotrphicum, which utilize these pathways, are morphologically similar to the carbonaceous filaments. On the contrary, such a large fractionation, up to ~40‰, is not produced via
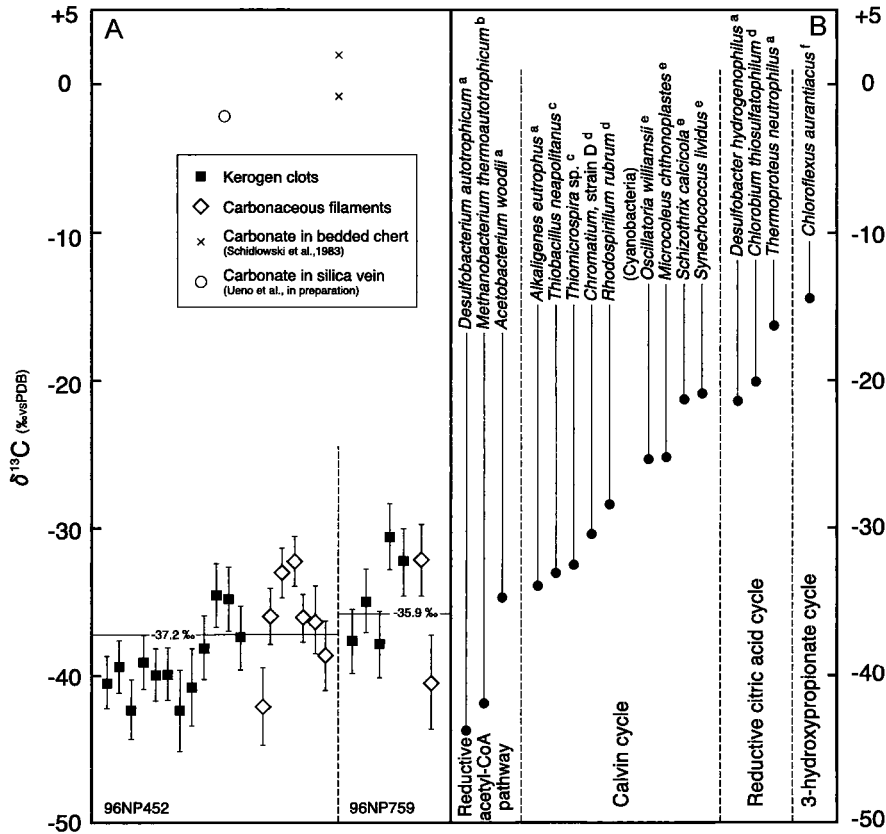
FIG. 9. A. Carbon isotope compositions of individual carbonaceous filaments and kerogen clots in silica vein samples, 96NP452 and 96NP759. Two horizontal lines indicate $\delta^{13}C$ values of bulk organic carbon determined by the conventional method (Ueno et al., in prep.), the precision of which is typically 0.1‰. Open circle and "x" symbols show $\delta^{13}C$ values of carbonate in silica vein of 96NP452 (Ueno et al., in prep.) and in bedded chert (Schidlowski et al., 1983), respectively. B. Observed maximum carbon isotope fractionations in four different carbon fixation pathways by modern autotrophic bacteria. Filled circles show recalculated $\delta^{13}C$ values for autotrophs assuming their use of atmospheric CO_2 ($\delta^{13}C = -8‰$), which is in equilibrium with carbonate ($\delta^{13}C = 0‰$) at 25°C (Mook et al., 1974). Sources of data for carbon isotope discrimination (superscript symbols after name of bacteria species): a = Preuss et al. (1989); b = Fuchs et al. (1979); c = Ruby et al. (1987); d = Sirevåg et al. (1977); e = Padue et al. (1976); and f = Holo and Sirevåg (1986).

the reductive citric acid cycle (Sirevåg et al., 1977; Preuss et al., 1989) and via the 3-hydroxypropionate cycle (Holo and Sirevåg, 1986; Menendez et al., 1999) unless CO_2 as a carbon source was not extraordinarily enriched in ^{12}C. In addition, cyanobacteria such as *O. williamsii*, *M. chthonoplastes*, *S. calcicola*, and *S. lividus* (Fig. 9B; Padue et al., 1976) also cannot produce such a large fractionation despite utilization of the Calvin cycle. Even though not all carbon fixation pathways in modern bacteria and their carbon isotope effects may be known, these isotopic signatures support the hypothesis that

autotrophic activity was already extant in the Archean.

In a single hand specimen, the $\delta^{13}C$ values of carbonaceous material including the filaments and kerogen clots vary by about 10‰. This scattering is beyond analytical precision (typically 2‰). The cause of this heterogeneity is not known. The kerogen clots and the filaments, although in the same sample, may have been derived from physiologically different organisms. Such variations of $\delta^{13}C$ values in a single thin section are also exhibited by Proterozoic fossil-bearing cherts (House et al., 2000), sug-

gesting that the isotopic heterogeneity of each minute fragment of the carbonaceous material including carbonaceous microfossils could have been maintained through post-depositional thermal maturation processes even as old as the Archean.

Conclusions

We determined the $\delta^{13}C$ values (–42 to –32‰) of newly found filamentous "probable microfossils" from Archean silica veins of the Warrawoona Group in Western Australia. These low $\delta^{13}C$ values strongly suggest that the filaments are composed of biologically fixed organic compounds. Such a large fractionation in carbon isotopes indicates that autotrophs, possibly utilizing the reductive acetyl-CoA pathway or the Calvin cycle, had already appeared in the Archean.

Acknowledgments

REFERENCES

Awramik, S. M., Schopf, J. W., and Walter, M. R., 1983, Filamentous fossil bacteria from the Archean of Western Australia: Precambrian Research, v. 20, p. 357–374.

_____, 1988, Carbonaceous filaments from North Pole, Western Australia: Are they fossil bacteria in Archaean stromatolites? A discussion: Precambrian Research, v. 39, p. 303–309.

Barghoorn, E. S., and Tyler, S. A., 1965, Microorganisms from the Gunflint chert: Science, v. 147, p. 563–577.

Brock, T. D., 1979, Biology of microorganisms: Englewood Cliffs, NJ: Prentice-Hall, Inc., 852 p.

Brocks, J. J., Logan, G. A., Buick, R., and Summons, R. E., 1999, Archean molecular fossils and the early rise of Eukaryotes: Science, v. 285, p. 1033–1036.

Buchanan, R. E., and Gibbons, N. E., 1974, Bergey's manual of determinative bacteriology, 8th ed.: Baltimore, MD: Williams and Wilkins, 1246 p.

Buick, R., 1984, Carbonaceous filaments from North Pole, Western Australia: Are they fossil bacteria in Archaean stromatolites?: Precambrian Research, v. 24, p. 157-172.

_____, 1988, Carbonaceous filaments from North Pole, Western Australia: Are they fossil bacteria in Archaean stromatolites? A reply: Precambrian Research, v. 39, p. 303–309.

_____, 1990, Microfossil recognition in Archean rocks: An appraisal of spheroids and filaments from a 3500 m.y. old chert-barite unit at North Pole, Western Australia: Palaios, v. 5, p. 441–491.

Buick, R., and Dunlop, J. S. R., 1990, Evaporitic sediments of Early Archean age from the Warrawoona Group, North Pole, Western Australia: Sedimentology, v. 37, p. 247–277.

Chacko, T., Mayeda, T. K., Clayton, R. N., and Goldsmith, J. R., 1991, Oxygen and carbon isotope fractionations between CO_2 and calcite: Geochimica et Cosmochimica Acta, v. 55, p. 2867–2882.

Craig, H., 1957, Isotopic standards for carbon and oxygen and correction factors for mass-spectrometric analysis of carbon dioxide: Geochimica et Cosmochimica Acta, v. 12, p. 133–149.

Degens, E. T., 1969, Biogeochemistry of stable carbon isotopes, in Organic geochemistry: New York, Springer, p. 304–329.

DesMarais, D. J., 1997, Isotopic evolution of the biogeochemical carbon cycle during the Proterozoic Eon: Organic Geochemistry, v. 27, p. 185–193.

Dunbar, C. E., and Rodgers, J., 1961, Principles of stratigraphy: New York: John Wiley and Sons, 248 p.

Dunlop, J. S. R., and Buick, R., 1981, Archaean epiclastic sediments derived from mafic volcanics, North Pole, Pilbara Block, Western Australia, in Archaean Geology: Second International Archean Symposium: Perth, Geological Society of Australia, Special Publication, p. 225–233.

Eichmann, R., and Schidlowski, M., 1975, Isotopic fractionation between coexisting organic carbon–carbonate pairs in Precambrian sediments: Geochimica et Cosmochimica Acta, v. 39, p. 585–595.

Eiler, J. M., Mojzsis, S. J., and Arrhenius, G., 1997, Carbon isotope evidence for early life: Nature, v. 386, p. 665.

Farquhar, G. D., Ehleringer, J. R., and Hubick, K. T., 1989, Carbon isotope discrimination and photosynthesis: Annual Review of Plant Physiology and Plant Molecular Biology, v. 40, p. 503–537.

Fuchs, G., 1989, Alternative pathways of autotrophic CO_2 fixation, in Autotrophic bacteria: New York, Springer Verlag, p. 365–382.

Fuchs, G., Thauer, R., Ziegler, H., and Stichler, W., 1979, Carbon isotope fractionation by *Methanobacterium*

thermoautotrophicum: Archives of Microbiology, v. 120, p. 135–139.

Hayes, J. M., 1994, Global methanotrophy at the Archean–Proterozoic transition, *in* Early life on Earth: New York, Columbia University Press, p. 220–236.

Hayes, J. M., Kaplan, I. R., and Wedeking, K. W., 1983, Precambrian organic geochemistry, preservation of the record, *in* Earth's earliest biosphere: Princeton, NJ, Princeton University Press, p. 93–134.

Hickman, A. H., 1973, The North Pole barite deposits, Pilbara Goldfield: Annual Report of Geological Survey of Western Australia for 1972, p. 57–60.

———, 1983, Geology of the Pilbara block and its environs: Geological Survey of Western Australia Bulletin, v. 127, p. 1–267.

———, 1990, Pilbara and Hamersley basin, Excursion guidebook, 3rd International Archean Symposium, p. 1–25.

Hiraishi, A., Umezawa, T., Yamamoto, H., Kato, K., and Maki, Y., 1999, Changes in quinone profiles of hot spring microbial mats with a thermal gradient: Applied and Environmental Microbiology, v. 65, p. 198–205.

Hoefs, J., and Frey, M., 1976, The isotopic composition of carbonaceous matter in a metamorphic profile from the Swiss Alps: Geochimica et Cosmochimica Acta, v. 40, p. 945–951.

Holo, H., and Sirevåg, R., 1986, Autotrophic growth and CO_2 fixation of *Chloroflexus aurantiacus*: Archives of Microbiology, v. 145, p. 173–180.

Holt, J. G., Krieg, N. R., Sneath, P. H. A., Staley, J. T., and Williams, S. T., 1994, Bergey's manual of determinative bacteriology, 9th ed.: Baltimore, MD: Williams and Wilkins, 787 p.

House, C. H., Schopf, J. W., McKeegan, K. D., Coath, C. D., Harrison, T. M., and Stetter, K. O., 2000, Carbon isotopic composition of individual Precambrian microfossils: Geology, v. 28, p. 707–710.

Isozaki, Y., Kabashima, T., Ueno, Y., Kitajima, K., Maruyama, S., Kato, Y., and Terabayashi, M., 1997, Early Archean mid-oceanic ridge rocks and early life in the Pilbara Craton, W. Australia: EOS (Transactions of the American Geophysical Union), v. 78, p. 399.

Knoll, A. H., 1999, A new molecular window on early life: Science, v. 285, p. 1025–1026.

Knoll, A. H., Strother, P. K., and Rossie, S., 1988, Distribution and diagenesis of microfossils from the Lower Proterozoic Duck Creek Dolomite, Western Australia: Precambrian Research, v. 38, p. 257–279.

Laws, E. A., Popp, B. N., Bidigare, R. R., Kennicutt, M. C., and Macko, S. A., 1995, Dependence of phytoplankton carbon isotopic composition on growth rate and $[CO_2]_{aq}$: Theoretical considerations and experimental results: Geochimica et Cosmochimica Acta, v. 59, p. 1131–1138.

Licari, G. R., 1978, Biogeography of the late Pre-Phanerozoic Beck Spring Dolomite of Eastern California: Journal of Paleontology, v. 54, p. 767–792.

Lipple, S. L., 1975, Definitions of new and revised stratigraphic units of the eastern Pilbara Region: Annual Report of the Geological Survey of Western Australia for 1974, p. 58–63.

Menendez, C., Bauer, Z., Huber, H., Gad'on, N., Stetter, K., and Fuchs, G., 1999, Presence of acetyl coenzyme A (CoA) carboxylase and propionyl-CoA carboxylase in autotrophic Crenarchaeota and indication for operation of a 3-hydroxypropionate cycle in autotrophic carbon fixation: Journal of Bacteriology, v. 181, p. 1088–1098.

Mook, W. G., Bommerson, J. C., and Staverman, W. H., 1974, Carbon isotope fractionation between dissolved bicarbonate and gaseous carbon dioxide: Earth and Planetary Science Letters, v. 22, p. 169–176.

Mojzsis, S. J., Arrhenius, G., McKeegan, K. D., Harrison, T. M., Nutman, A. P., and Friend, C. R. L., 1996, Evidence for life on Earth before 3,800 million years ago: Nature, v. 385, p. 55–59.

Nijman, W., de Bruijne, K. H., and Valkering, M. E., 1998, Growth fault control of Early Archaean cherts, barite mounds and chert-barite veins, North Pole Dome, Eastern Pilbara, Western Australia: Precambrian Research, v. 88, p. 25–52.

Ohmoto, H., and Kerrick, D., 1977, Devolatilization equilibria in graphitic systems: American Journal of Science, v. 277, p. 1013–1044.

Padue, J. W., Scalan, R. S., Van Baalen, C., and Parker, P. L., 1976, Maximum carbon isotope fractionation in photosynthesis by blue-green algae and a green alga: Geochimica et Cosmochimica Acta, v. 40, p. 309–312.

Peters, K. E., Rohrback, B. G., and Kaplan, I. R., 1981, Carbon and hydrogen stable isotope variations in kerogen during laboratory-simulated thermal maturation: American Association of Petroleum Geologists Bulletin, v. 65, p. 501–508.

Popp, B. N., Laws, E. A., Bidigare, R. R., Dore, J. E., Hanson, K. L., and Wakeham, S. G., 1998, Effect of phytoplankton cell geometry on carbon isotopic fractionation: Geochimica et Cosmochimica Acta, v. 62, p. 69–77.

Preuss, A., Schauder, R., Fuchs, G., and Stichler, W., 1989, Carbon isotope fractionation by autotrophic bacteria with three different CO_2 fixation pathways: Zeitschrift für Naturforschung, v. 44c, p. 397–402.

Richards, J. R., Fletcher, I. R., and Blockley, J. G., 1981, Pilbara galenas: Precise isotopic assay of the oldest Australian leads, model ages and growth curve implications: Mineralium Deposita, v. 16, p. 7–30.

Ruby, E. G., Jannasch, W., and Deuser, W. G., 1987, Fractionation of stable carbon isotopes during chemoautotrophic growth of sulfur-oxidizing bacteria: Applied and Environmental Microbiology, v. 53, p. 1940–1943.

Scheele, N., and Hoefs, J., 1992, Carbon isotope fractionation between calcite, graphite and CO_2: An experimental study: Contributions to Mineralogy and Petrology, v. 112, p. 35–45.

Schidlowski, M., Hayes, J. M., and Kaplan, I. R., 1983, Isotopic inferences of ancient biochemistries: Carbon, sulfur, hydrogen, and nitrogen, in Earth's earliest biosphere: Princeton, NJ, Princeton University Press, p. 149–186.

Schopf, J. W., 1968, Microflora of the Bitter Springs Formation, late Precambrian, central Australia: Journal of Paleontology, v. 42, p. 651–688.

———, 1992, Paleobiology of the Archean, in The Proterozoic biosphere: A multidisciplinary study: Cambridge, UK, Cambridge University Press, p. 25–39.

———, 1993, Microfossils of the Early Archean Apex Chert: New evidence of the antiquity of life: Science, v. 260, p. 640–646.

———, 1998, Tracing the roots of the Universal Tree of Life, in The molecular origins of life: New York, Cambridge University Press, p. 336–362.

Schopf, J. W., and Packer, B. M., 1987, Early Archean (3.3 billion to 3.5-billion-year-old) microfossils from Warrawoona Group, Australia: Science, v. 237, p. 70–73.

Schopf, J. W., and Walter, M. R., 1983, Archean microfossils: New evidence of ancient microbes, in Earth's earliest biosphere: Princeton, NJ, Princeton University Press, p. 214–239.

Sirevåg, R., Buchanan, B. B., Berry, J. A., and Troughton, J. H., 1977, Mechanisms of CO_2 fixation in bacterial photosynthesis studied by the carbon isotope fractionation technique: Archives of Microbiology, v. 112, p. 35–38.

Stetter, K. O., 1994, The lesson of Archaebacteria, in Early life on Earth: New York, Columbia University Press, p. 143–160.

Strauss, H., and Moore, T. B., 1992, Abundances and isotopic compositions of carbon and sulfur species in whole rock and kerogen samples, in The Proterozoic biosphere: A multidisciplinary study: Cambridge, UK, Cambridge University Press, p. 709–798.

Summons, R. E., and Hayes, J. M., 1992, Principles of molecular and isotopic biogeochemistry, in The Proterozoic biosphere: A multidisciplinary study: Cambridge, UK, Cambridge University Press, p. 83–93.

Summons, R. E., Jahnke, L. L., Hope, J. M., and Logan, G. A., 1999, 2-Methylhopanoids as biomarkers for cyanobacterial oxygenic photosynthesis: Nature, v. 400, p. 554–557.

Thorpe, R. I., Hickman, A. H., Davis, D. W., Mortensen, J. K., and Trendall, A. F., 1992a, Constraints to models for lead evolution from precise zircon U-Pb geochronology for the Marble Bar region, Pilbara Craton, Western Australia, in The Archaean: Terrains, processes and metallogeny: The University of Western Australia, Publication 9, p. 395–406.

———, 1992b, U-Pb zircon geochronology of Archean felsic units in the Marble Bar region, Pilbara Craton, Western Australia: Precambrian Research, v. 56, p. 169–189.

Ueno, Y., Yoshioka, H., Maruyama, S., and Isozaki, Y., in preparation, Carbon and nitrogen isotope ratios of kerogen in Archean silica veins of North Pole area, Western Australia.

Van Kranendonk, M., 1999, North Shaw, W. A. Sheet 2755: Western Australia Geological Survey, 1: 100,000 Geological Series.

Walsh, M. M., 1992, Microfossils and possible microfossils from the early Archean Onverwacht Group, Barberton Mountain Land, South Africa: Precambrian Research, v. 54, p. 271–293.

Walter, M. R., 1983, Archean stromatolites: Evidence of the Earth's earliest benthos, in Earth's earliest biosphere: Princeton, NJ, Princeton University Press, p. 187–213.

Watanabe, Y., Naraoka, H., Wronkiewicz, D. J., Condie, K. C., and Ohmoto, H., 1997, Carbon, nitrogen, and sulfur geochemistry of Archean and Proterozoic shales from the Kaapvaal Craton, South Africa: Geochimica et Cosmochimica Acta, v. 61, p. 3441–3459.

Woese, C. R., 1987, Bacterial evolution: Microbiological Review, v. 51, p. 221–271.

Wopenka, B., and Pasteris, J. D., 1993, Structural characterization of kerogens to granulite-facies graphite: Applicability of Raman microprobe spectroscopy: American Mineralogist, v. 78, p. 533–557.

Yamamoto, H., Hiraishi, A., Kato, K., Chiura, H. X., Maki, Y., and Shimizu, A., 1998, Phylogenetic evidence for the existence of novel thermophilic bacteria in hot spring sulfur-turf microbial mats in Japan: Applied and Environmental Microbiology, v. 64, p. 1680–1687.

Yui, T. F., Huang, E., and Xu, J., 1996, Raman spectrum of carbonaceous material: A possible metamorphic grade indicator for low-grade metamorphic rocks: Journal of Metamorphic Geology, v. 14, p. 115–124.